Widespread distribution of the BpfA-carrying bacteria involved in the bisphenol F degradation in Pseudomonadota and Actinomycetota

Changchang Wang[a,1], Mingliang Zhang[a,1], Yanni Huang[a], Qian Li[a], Junqiang Hu[a], Kaihua Pan[a], Qian Zhu[a], Wankui Jiang[b], Jiguo Qiu[a], Xin Yan[a*], Qing Hong[a*]

[a] Department of Microbiology, College of Life Sciences, Nanjing Agricultural University, Key Laboratory of Agricultural and Environmental Microbiology, Ministry of Agriculture and Rural Affairs, Nanjing 210095, China.

[b] State Key Laboratory of Materials-Oriented Chemical Engineering, College of Biotechnology and Pharmaceutical Engineering, Nanjing Tech University, Nanjing 211800, PR China.

[1] Contributed equally to this paper.

* Author for correspondence: Xin Yan and Qing Hong

E-mail address: yanxin@njau.edu.cn. and hongqing@njau.edu.cn.

Tel: +86-25-84396685, Fax: +86-25-84395326

ABSTRACT

The global use of bisphenol F (BPF) has led to widespread environmental contamination, posing significant threats to ecosystems and human health. However, the genes involved in BPF degradation remained unknown. In this study, a novel oxidase gene, *bpfA*, was obtained from strain *Microbacterium* sp. F2 through a four-step purification strategy. BpfA is classified as a member of the 4-phenol oxidizing (4PO) subfamily and contains a conserved FAD-binding domain (Asp152 and His393) as well as a Tyr-Tyr-Arg triad (Tyr93, Tyr474, Arg475). BpfA catalyzes the conversion of BPF to 4,4′-dihydroxydibenzophenone (DHBP) through a series of three consecutive reactions. In addition, BpfA exhibits catalytic activity towards 4-alkylphenols, such as vanillyl alcohol (VA), 4-n-propylguaiacol (4PG), and 4-(methoxymethyl)phenol (4MOP). BpfA homologs are widely distributed in the environment, particularly in soil. Bioinformatics-based taxonomic profiling revealed that BpfA homologs are widely distributed in metagenomes from cultivated land and forests, mainly belonging to Pseudomonadota and Actinomycetota. This study enhances our understanding of the microbial degradation mechanism of BPF, elucidates the catalytic function of the novel oxidase gene *bpfA* and its distribution pattern in the environment, and provides important insights into the evolutionary origin of BPF degradation genes and the targeted mining of environmental microbial resources.

KEYWORDS: Bisphenol F, Biodegradation, FAD-binding oxidoreductase BpfA, *Microbacterium* sp. F2, Distribution pattern.

Introduction

Bisphenols (BPs) are one of the important chemical raw materials for the synthesis of high-molecular-weight materials and are widely used in various consumer products, including bisphenol A (BPA), bisphenol F (BPF), bisphenol B (BPB), bisphenol S (BPS), and bisphenol AF (BPAF). However, toxicological studies have shown that BPA has endocrine-disrupting effects and may trigger a variety of health problems, such as cancer [1], reproductive disorders [2,3], and obesity [4,5]. As one of the main substitutes for BPA, the usage of BPF has increased year by year, and it has become a new, widely-present pollutant in water bodies [6]. BPF enters aquatic, soil, and atmospheric environments via industrial effluent discharge, plastic product degradation, and landfill leachate and has been widely detected globally [7,8]. BPF contamination in East Asian aquatic systems reaches notable levels, exceeding 1000 ng/L in rivers and seawater across Japan, Korea, and China; the highest concentration (2850 ng/L) was detected in Tokyo's Tamagawa River [9-11]. Moreover, the breast milk samples collected from 181 healthy women across various provinces and cities in China revealed an average BPF concentration of 0.107 μg/L [12]. This suggests that BPF, in addition to its widespread presence in the aquatic environment, may also pose risks to human health through bioaccumulation.

BPF has toxic effects on organisms. Exposure to 0.5 mM BPF during the embryonic stage of fruit flies reduced the number of neuroblasts and intermediate neural progenitor cells, leading to an imbalance in the neuron-to-glial cell ratio. This disrupted the proliferation of neural stem cells, resulting in neurodevelopmental

toxicity and abnormal larval behavior [13]. Through transcriptomic and metabolomic studies, it was found that exposure to 1.0 μM BPF upregulated the expression of pro-inflammatory cytokines (such as IL-17A and TNF-α) in human colonic epithelial cells (NCM460), while downregulating tight junction proteins (ZO-1 and CLDN1), thereby disrupting intestinal barrier function [14]. In addition, adult male zebrafish exposed to BPF concentrations of 500 nM and 2500 nM exhibited significant reductions in sperm count, decreased levels of serum testosterone (T), and increased levels of vitellogenin (VTG) in the liver, indicating that BPF has endocrine-disrupting effects on adult male zebrafish [15].

Several bacterial strains capable of growing with BPF have recently been identified, including *Pseudomonas* sp. HS-2 [16], *Pseudomonas* sp. ZH-FAD [17], *Sphingobium yanoikuyae* FM-2 [18], *Sphingobium yanoikuyae* TYF-1 [19], *Arthrobacter* sp. YC-RL1 [20], and *Microbacterium* sp. F2 [21]. The identification of similar intermediates in the BPF degradation process among strains from various genera has led to the proposal of a common catabolic pathway (Fig. S1). This pathway involves the initial hydroxylation of the BPF carbon bridge to form (4-hydroxyphenyl)methanol (BHPM), followed by dehydrogenation to produce 4,4´-dihydroxydibenzophenone (DHBP). Subsequently, the Baeyer-Villiger reaction occurs between the two phenolic rings to generate 4-hydroxybenzoic acid-4-hydroxyphenyl ester (HPHB), which is hydrolyzed into *p*-hydroxybenzoic acid (PHBA) and hydroquinone (HQ). These compounds are further degraded to provide carbon sources for the growth of the strains. Although several BPF-degrading bacterial strains have

been reported, the specific genes involved in the conserved BPF metabolic pathway remain unknown. Elucidating these BPF degradation genes is crucial for understanding the transformation and ultimate fate of BPF in the environment.

In the current study, a novel oxidase gene, *bpfA*, was identified in the previously isolated BPF-degrading strain *Microbacterium* sp. F2, which catalyzes the conversion of BPF to DHBP through three consecutive reactions. The classification of the *bpfA* gene and its distribution in various environments worldwide were analyzed. These results provide novel perspectives on the variety of BPF degradation genes across distinct microbial strains.

Materials and methods

Chemicals and media

Bisphenol F (BPF), bisphenol E (BPE), vanillyl alcohol (VA), 4,4′-dihydroxybenzophenone (DHBP), 4-*n*-propylguaiacol (4PG), 4-hydroxyphenyl 4-hydroxybenzoate (HPHB), 4-(Methoxymethyl) phenol (4MOP), *p*-hydroxybenzoic acid (PHBA), and 1,4-hydroquinone (HQ) were purchased from Shanghai Macklin Biochemical Technology Co., Ltd (Shanghai, China). BPF degradation experiments were performed in a mineral salts medium (MSM, pH 7.0). The bacterial strains used in this study were cultured in lysogeny broth (LB, pH 7.0) [21].

Strains, plasmids, and cultural conditions

Details of the bacterial strains and plasmids utilized in this study are provided in Supplementary Table S1. *Microbacterium* sp. F2 was cultured in LB broth or MSM at 30°C and 180 rpm, unless otherwise specified. *Escherichia coli* strains were cultured in

106 LB broth at 37°C and 200 rpm.

107 BPF degradation assay

108 Strain F2 was initially cultured in LB medium for 24 h, followed by centrifugation
109 at 4°C (5,000 × *g*, 5 min). The harvested cells were washed three times with sterile
110 MSM. The cells, adjusted to an OD_{600} of 1.0, were then inoculated into MSM
111 supplemented with 0.10 mM BPF and incubated at 30°C. Aliquots (1 mL) were taken
112 every 2 h and analyzed via high-performance liquid chromatography (HPLC) to
113 quantify BPF concentrations. A control experiment was conducted using MSM without
114 strain F2 under identical conditions. All treatments were performed in triplicate.

115 To prepare BPF-induced cells, strain F2 cells cultured in LB medium were
116 harvested, washed three times with sterile MSM, and inoculated into MSM containing
117 0.10 mM BPF. When half of the BPF was degraded, the BPF-induced cells were
118 collected. For BPF-induced cell extracts, the cells were washed twice with 20 mM Tris-
119 HCl buffer (pH 8.0), resuspended in 15 mL of the same buffer, and lysed using an
120 ultrasonic processor (UH-650B, Auto Science) in an ice bath. The lysates were then
121 centrifuged at 12,000 × g for 20 min at 4 °C. For the BPF degradation experiments,
122 a 3 mL reaction mixture containing 0.10 mM BPF and 1 mL of cell lysate was prepared
123 in a 20 mM Tris-HCl buffer (pH 8.0) at 30°C. The reaction was terminated immediately
124 by boiling for 5 min after completion. Samples were collected every 10 min and
125 analyzed by HPLC to measure the concentration of BPF.

126 Sequencing and analysis

127 Genomic DNA from strain F2 was extracted using a commercial kit (TIANGEN

128 BIOTECH Co., LTD, Beijing, China). The genome of strain F2 (accession number:
129 JBNVBV000000000) was sequenced by Majorbio Biomedical Technology Co., Ltd
130 (Shanghai, China). Gene prediction and annotation were carried out using Glimmer
131 3.02 and RAST (Rapid Annotation Subsystem Technology) database
132 (https://rast.nmpdr.org/) [22].

133 **Purification of BpfA from the cell extract of strain F2**

134 The purification was conducted at 0-4°C using a 20 mM Tris-HCl buffer (pH 8.0).
135 The detailed protocol followed the methods previously reported [45]. The protein band
136 visualized on SDS-PAGE (Fig. S3, lane 6) was excised and subjected to peptide mass
137 spectrometry analysis. The resulting peptide fragments were matched against the
138 annotated genes from strain F2 to pinpoint sequences with high homology.
139 Subsequently, the resulting protein sequences underwent a BLASTP search against the
140 NCBI non-redundant protein (NR) database. Based on these analyses, the gene
141 encoding FAD-binding oxidoreductase, *bpfA*, was identified as a potential candidate for
142 catalyzing BPF and was selected for further protein expression and *in vitro* BPF
143 degradation assays.

144 Bioinformatic Analysis

145 A BLASTP search was conducted using the BpfA sequence (PV658135) from
146 *Microbacterium* sp. F2 as the query sequence, targeting all genomes within the NCBI
147 database to uncover BpfA homologues. The sequence similarity network (SSN) was
148 created utilizing the Enzyme Function Initiative Enzyme Similarity Tool (EFI-EST)
149 [23]. An all-by-all BLAST was performed on the sequences, and the SSN was

150 subsequently built based on an alignment score cutoff of 90. Visualization of the SSN
151 was accomplished with Cytoscape [24]. For the phylogenetic analysis of BpfA,
152 homologous sequences were retrieved from the NCBI NR database. These sequences
153 were aligned using the ClustalX [25], and the resultant alignment was transferred to
154 MEGA (version 11.0) [26] for further processing. The phylogenetic tree was
155 subsequently generated employing the neighbor-joining algorithm.

156 Previously, species-level genome bins (SGBs) were constructed from 3,304 soil
157 metagenomes, ensuring medium to high quality standards (with completeness
158 exceeding 50% and contamination below 10%). Further details are available at the
159 Global Soil MAGs Project website [27]. These SGBs were classified using GTDB-Tk
160 (version 1.6.0), and the BpfA protein was identified through Prodigal, with stringent
161 criteria (identity greater than 35%, e-value less than 1×10^{-5}, and subject coverage
162 over 95%) [28]. To explore the global distribution of BpfA, amino acid sequences from
163 the SGBs were obtained and analyzed via Diamond (v2.1.6). By integrating
164 classification data from SGBs and GTDB, a comprehensive analysis of BpfA species
165 distribution was accomplished [29]. Additionally, the classification of target genomes
166 as either isolated or uncultured (including metagenomic assembly genomes and single
167 amplified genomes) was determined by searching both GTDB and NCBI RefSeq [30].

168 Gene expression and purification of the recombinant enzyme

169 The primer pair *bpfA*$_{F2}$-F and *bpfA*$_{F2}$-R (Supporting Information Table S2) was
170 used to amplify the *bpfA* gene from strain F2. The amplified *bpfA* gene was cloned into
171 the NdeI/XhoI-digested pET29a(+) plasmid via homologous recombination, resulting

172 in the recombinant plasmid pET-*bpfA*. This plasmid was then introduced into
173 *Escherichia coli* BL21(DE3) to create the expression strain *E. coli* BL21(pET-*bpfA*).
174 The strain *E. coli* BL21(pET-*bpfA*) was inoculated into LB containing 50 mg/L
175 kanamycin and cultured until the cell density reached an OD_{600} of 0.5-0.6, at which
176 point 0.2 mM IPTG was added to induce protein expression for 12 h at 16°C. Cells
177 were centrifuged and lysed using an ultrasonic processor. The supernatant was obtained
178 by centrifugation at 4°C and then passed through a Ni-NTA column (Sangon, Shanghai,
179 China). A series concentrations of imidazole were used to elute the column and purify
180 the recombinant protein. The purified protein was then dialyzed overnight in Tris-HCl
181 buffer (pH 8.0) and analyzed by SDS-PAGE. A BCA kit from Vazyme Biotech Co., Ltd
182 (Nanjing, China) was used to determine the protein concentration.

183 The genes *eugO* from *Rhodococcus jostii* RHA1 (Q0SBK1), *vaO* from *Penicillium*
184 *simplicissimum* CBS 170.90 (P56216), and FAD-binding oxidoreductase gene *fbO*
185 from *Sphingobium* sp. W15 (PV658134) were synthesized from Nanjing Qingke
186 Biotechnology Co., Ltd (Nanjing, China). The protein expression and purification
187 methods for EUGO, VAO, and FAD-binding oxidoreductase were similar to those
188 described above.

189 Enzyme activity assays

190 Enzymatic assays for BpfA were performed at 30°C for 2 h in a 1 mL reaction
191 mixture containing 20 mM Tris-HCl buffer (pH 8.0), 0.10 mM BPF, and 3.0 μM BpfA.
192 The enzymatic reactions were terminated by boiling for 5min. Enzyme activity was
193 quantified as the amount of enzyme needed to convert 1 μmol of BPF per minute,

194 defined as one unit.

195 To determine the optimal reaction temperature, BpfA's activity was tested at
196 various temperatures, spanning from 20°C to 50°C in 5°C increments. The thermal
197 stability of BpfA was evaluated by subjecting the enzyme to different temperatures for
198 30 min, after which the residual activity was assessed under the specified assay
199 conditions. The non-heated enzyme was used as the control (100%). The optimal
200 reaction pH was determined using a variety of buffers: 20 mM Citrate-Phosphate buffer
201 (pH 4.0 to 6.0), 20 mM Tris-HCl buffer (pH 6.0 to 8.0), and 20 mM glycine-NaOH
202 buffer (pH 8.0 to 10.0). The pH stability of BpfA was examined by incubating the
203 enzyme at 4°C for 30 min in buffers with diverse pH, with residual activities
204 subsequently measured. Samples were collected prior to complete substrate
205 consumption. A reaction mixture devoid of the enzyme served as a negative control.
206 The activity of the reference enzyme was designated as 100%, and the relative activities
207 of each reaction were determined as a percentage relative to the reference.

208 To evaluate the substrate specificity of BpfA, the enzyme was tested with various
209 substrates (BPE, VA, 4PG, and 4MOP) at a concentration of 0.10 mM each, under the
210 reaction conditions described above. The activity assays for EUGO, VAO, and FBO
211 were similarly performed following the same procedures.

212 Site-directed mutagenesis

213 Mutations at specific sites within the *bpfA* gene were engineered via overlap
214 extension PCR. The primer pairs Y93A-F/R, Y474A-F/R, R475A-F/R, D152A-F/R,
215 and H393A-F/R were used to introduce the mutation sites (Table S2). The site-directed

216 mutagenesis amplification was carried out following the protocol provided with the
217 site-directed mutagenesis kit (Vazyme Biotech Co., Ltd., China). The resulting PCR
218 products were purified by gel extraction and ligated into pET-29a(+) vector, following
219 the previously described method. The activity assessment of the mutant proteins was
220 carried out using the previously detailed procedures.

221 **Analytical methods**

222 Enzyme assay samples were boiled for 5min and subsequently centrifuged at
223 12,000 × *g* for 5 min. The resulting supernatant was passed through a 0.2-mm-pore-size
224 membrane prior to further analysis of the products. The detection and quantification of
225 BPF and its metabolites in enzyme assay samples were performed using HPLC [21].
226 The identification of BpfA and its metabolites in enzyme assay samples was achieved
227 using mass spectrometry on an AB SCIEX Triple TOF 5600 [21].

228 **Results and discussion**

229 **Cloning and sequence analysis of *bpfA* gene.**

230 *Microbacterium* sp. F2 has been reported to use BPF as the sole carbon source for
231 growth, with BPF degradation being induced by BPF itself [21]. Furthermore, cell
232 extract from BPF-induced strain F2 completely degraded 0.10 mM BPF, regardless of
233 whether NADPH, NADH, and FAD were introduced (Fig. S2). Therefore, the gene
234 encoding the initial step of BPF degradation can be obtained from the cell extract of
235 strain F2 via protein purification techniques. A four-stage purification protocol was
236 utilized to refine the BPF-degrading enzyme from the cell extract of BPF-induced strain
237 F2. Initially, the specific activity in the cell extract from strain F2 was determined to be

238 0.37 U/mg protein. Following the four purification steps, the specific activity of the
239 final fraction rose to 14.74 U/mg, with a 24.15-fold increase in protein concentration
240 and a recovery rate of 4.76% (Table S3). Subsequent SDS-PAGE analysis of the final
241 fraction showed a single protein band (Fig. S3), which was excised and subjected to
242 peptide mass spectrometry analysis. The analysis yielded sequences of fifteen peptide
243 fragments, which were then matched against all annotated genes within strain F2
244 (JBNVBV000000000) (Table S4). Subsequently, all candidate genes predicted to
245 degrade BPF were annotated and experimentally validated. A FAD-binding
246 oxidoreductase-encoding gene, *orf1733* (ACQVDU_06965), demonstrated BPF-
247 degrading activity and was designated as *bpfA*, which was selected for further studies.
248 The *bpfA* gene (1,599 bp) encodes a 532-amino acid oxidase that shares 30%–55%
249 identity with FAD-binding oxidoreductases from various genera (Non-redundant
250 Protein Sequences Database). BpfA is classified within the flavoprotein oxidase
251 superfamily [31,32]. A sequence similarity network (SSN) analysis indicates that BpfA
252 is a member of the vanillyl alcohol oxidase (VAO) flavoprotein family (PF01565)
253 within this superfamily (Fig. 1A). BpfA shows 33% to 42% sequence identity with three
254 biochemically characterized oxidoreductases from *Rhodococcus jostii* RHA1 (vanillyl-
255 alcohol oxidase EUGO [Q0SBK1]; 41.14% identity) [33], *Penicillium simplicissimum*
256 CBS 170.90 (vanillyl-alcohol oxidase VAO [P56216]; 37.50% identity) [34], and
257 *Pseudomonas putida* NCIMB 9869 (*p*-cresol methylhydroxylase PCMH [P09788.3];
258 33.20% identity) [35]. These three enzymes are members of the VAO flavoprotein
259 family, which is characterized by a conserved FAD-binding domain [36] and a Tyr-Tyr-

260 Arg triad essential for substrate binding [37]. Additionally, the VAO flavoprotein family
261 (PF01565) is further divided into 11 subfamilies [37]. BpfA clusters with the reported
262 members of the 4-phenol oxidizing (4PO) subfamily, including EUGO (Q0SBK1),
263 PCMH (P09788.3), and VAO (P56216), suggesting that these proteins may have a
264 closer phylogenetic relationship and similar functions (Fig. 1B). BpfA and other
265 members of the 4PO subgroup, including EUGO, PCMH, and VAO, share five
266 conserved motifs (Fig. S4) [38]. The residues in the 4PO-motif-1 form a loop that
267 closely interacts with the FAD cofactor. Notably, one of the tyrosine residues (Tyr93),
268 which is essential for substrate deprotonation, is situated within this loop. The 4PO-
269 motif-5 also forms a loop that includes the other two residues, Tyr474 and Arg475,
270 involved in substrate deprotonation. Furthermore, the amino acids Asp152 and His393
271 are involved in forming a covalent bond with FAD, which is critical for the enzyme's
272 redox properties. This covalent binding significantly enhances the redox potential of
273 the enzyme [39], thereby accelerating the rate of FAD reduction by the substrate and,
274 consequently, enhancing the overall reaction rate [39].

275 **Functional identification of BpfA.**

276 The purified BpfA protein displayed a pale yellow and showed a single band on
277 SDS-PAGE, with an observed molecular mass of 59.9 kDa, which closely aligns with
278 the theoretical molecular mass of 58.8 kDa (Fig. 2A). Purified BpfA was able to
279 completely degrade 0.10 mM of BPF *in vitro* within 40 min. During the degradation of
280 BpfA, four metabolites were identified (namely compound I, II, III, and IV) (Fig. 2B).
281 The peak height of compound I (5.000 min) continuously decreased and completely

282 disappeared at 40 min. After 20 min, compound II (3.998 min), compound III (2.708
283 min), and compound IV (3.703 min) appeared simultaneously with the degradation of
284 compound I. However, compound II only appeared briefly before rapidly disappearing.
285 Subsequently, compound III was gradually converted to compound IV and completely
286 disappeared after 60 min. Ultimately, the peak height of compound IV continuously
287 increased and remained unchanged. These compounds were identified by HPLC-MS as
288 BPF (compound I, Fig. 2C), 4-[(4-hydroxyphenyl)methylene]cyclohexa-2,5-dien-1-
289 one (HMC) (compound II, Fig. 2D), BHPM (compound III, Fig. 2E), and DHBP
290 (compound IV, Fig. 2F). Additionally, we detected the production of 0.189 mM
291 hydrogen peroxide (H_2O_2) during the degradation of 0.10 mM BPF by BpfA using the
292 H_2O_2 colorimetric method [40], with a ratio of approximately 1:2 (Fig. S5).

293 The identified metabolites led to the proposal of a BPF degradation pathway
294 mediated by BpfA (Fig. 2G). Initially, the phenolic -OH group of BPF is deprotonated
295 by two conserved tyrosine residues of BpfA (Y93 and Y474). The electron density is
296 then conducted through the aromatic ring, extruding a hydride ion (H^-) from the α-
297 position, which is accepted by the isoalloxazine ring of the oxidized flavin cofactor.
298 The resulting quinone methide intermediate (HMC) then acts as an electrophile,
299 undergoing nucleophilic addition with a water molecule catalyzed in the BpfA´s active
300 site, leading to the formation of the hydroxylated product (BHPM). Finally, BHPM
301 undergoes further dehydrogenation to generate DHBP. Meanwhile, FAD is reoxidized
302 by molecular oxygen, which is converted to H_2O_2. The initial deprotonation of the
303 phenolic hydroxyl group of the substrate is a crucial step in this mechanism, as it

304 facilitates the hydride transfer reaction by promoting the formation of the *para*-quinone
305 methide intermediate. The same effect has been observed in VAO and EUGO [41,42].
306 In this study, BpfA catalyze the sequential transformation of BPF into the quinone
307 methide intermediate HMC, BHPM, and DHBP (Fig. 2), which differs from the BPF
308 degradation pathway proposed in strain F2, in which BPF was metabolized into BHPM
309 and DHBP without the detection of the intermediate HMC [21]. According to the
310 previously reported VAO catalytic mechanism, the key product intermediate, quinone
311 methide, is transiently formed and allows for the rapid occurrence of several different
312 oxidation reactions [41,42]. We speculate that the quinone methide intermediate HMC
313 may be rapidly converted to BHPM in strain F2, and thus cannot be captured by HPLC.
314 In this study, purified BpfA is used to catalyze BPF *in vitro* and detected HMC through
315 multiple consecutive samplings. In short, The proposed BPF degradation pathway in
316 strain F2 was described at the cellular level but lacked genetic or enzymatic evidence.
317 However, this study elucidates the BPF degradation process at the enzymatic and
318 genetic levels and proposes a modified BPF metabolic pathway compared to that by
319 Wang et al. [21].
320 **BpfA and 4PO subfamily proteins**
321 To investigate the potential distribution of BpfA across different strains, we
322 searched the NCBI NR database for homologs with a coverage of no less than 95% and
323 at least 30% amino acid sequence identity. Consequently, 49 gene pairs belonging to
324 the 4PO subfamily were identified from three bacterial phyla, specifically from
325 Pseudomonadota (12), Actinomycetota (27), and Ascomycota (10) (Fig. 3A). The BpfA

326 homologs originate from soil, sediments, clinical specimens, wastewater, faeces,
327 pulping wastewater, oil-well water-associated microorganisms, indicating their
328 ubiquity in the environment. Phylogenetic tree analysis shows that BpfA, EUGO, VAO,
329 and PCMH are located on different branches, suggesting that they may not have evolved
330 directly from a single common ancestor but rather may have undergone different
331 branching events during the course of evolution. In order to determine if these BpfA
332 homologous genes were functional, we synthesized three genes from Ascomycota,
333 Actinomycetota and Pseudomonadota: EUGO (Q0SBK1; *Rhodococcus jostii* RHA1;
334 coverage 98%; identity 41.14%), VAO (P56216; *Penicillium simplicissimum* CBS
335 170.90; coverage 96%; identity 37.50%), and FAD-binding oxidoreductase FBO
336 (PV658134; *Sphingobium* sp. W15; coverage 97%; identity 39.46%), for the purpose
337 of expressing recombinant proteins in *E. coli*. Given that PCMH from *Pseudomonas*
338 *putida* NCIMB 9869 (Pseudomonadota) is a two-component protein with an $\alpha 2\beta 2$
339 structure, comprising an α-subunit (PchF) and a β-subunit (PchC) to function [35], and
340 considering that the reported EUGO and VAO are both single-component proteins, this
341 study did not consider synthesizing PCMH for subsequent functional validation.

342 In the absence of FAD, VAO, EUGO, and FBO exhibited weak activity against
343 BPF, with the specific activity of BpfA being 2452, 2907, and 3672 times higher than
344 that of VAO, EUGO, and FBO, respectively (Fig. 3B). In the presence of FAD, the
345 specific activity of BpfA was 2381, 2809, and 2104 times higher than that of VAO,
346 EUGO, and FBO, respectively (Fig. 3B). There was no significant difference in the
347 catalytic activity of VAO and EUGO against BPF, regardless of the presence or absence

348 of FAD. Compared with VAO and EUGO, the addition of FAD significantly enhanced
349 the catalytic activity of FBO against BPF. Further analysis revealed that FBO (D to G
350 mutation) each had only one amino acid residue involved in FAD binding altered (Fig.
351 3A). Therefore, the addition of FAD was required for FBO to exhibit higher catalytic
352 activity. The above results indicate that members of the 4PO subfamily proteins exhibit
353 catalytic activity against BPF.

354 **Biochemical characterization of BpfA.**

355 The specific BpfA activity was 14.71 U mg^{-1} protein for BPF (Fig. 3B). The highest
356 BPF activity was observed at a temperature of 30°C and a pH of 8.0 (Fig. S6). When
357 the enzyme was exposed to 40°C for 30 min, it maintained over 80% of its initial
358 activity. In contrast, incubation at 45°C for the same duration resulted in significant
359 instability, with the enzyme retaining only 30% of its initial activity (Fig. S6A). BpfA
360 exhibits high activity at a pH of 8.0, with its activity dropping below 20% at pH less
361 than 5.0. When stored for 30 min at pH ranging from 7.0 to 10.0, its activity remains at
362 70% (Fig. S6B).

363 BpfA exhibits catalytic activity against other *para*-substituted phenolic compounds,
364 including vanillyl alcohol (VA), 4-n-propylguaiacol (4PG), and 4-
365 (methoxymethyl)phenol (4MOP) (Fig. 3C). The specific activity of BpfA against BPF
366 is 249, 2.09, and 210 times higher than that against VA, 4PG, and 4MOP, respectively.
367 However, BpfA does not exhibit catalytic activity against bisphenol E (BPE), which
368 has a structure similar to BPF (Fig. S7), indicating that the two active hydrogen atoms
369 on the α-position carbon of *para*-substituted phenolic compounds are crucial for BpfA

370 to function.

371 Moreover, the Tyr-Tyr-Arg triad and conserved FAD-binding domain (Y93, Y474,
372 R475, D152, and H393) of BpfA was replaced by alanine, resulting in five variants
373 ($BpfA^{Y93A}$, $BpfA^{Y474A}$, $BpfA^{R475A}$, $BpfA^{D152A}$, and $BpfA^{H393A}$) (Fig. S8). Among the
374 five mutants, only the purified $BpfA^{Y474A}$ and $BpfA^{H393A}$ exhibited the same pale yellow
375 as the wild-type BpfA (Fig. S8A). $BpfA^{Y474A}$ and $BpfA^{H393A}$ retained 6.6% and 71.1%
376 of their activity against BPF, respectively, while the other mutants completely lost their
377 catalytic activity against BPF (Fig. S8B). This indirectly highlights the significance of
378 the Tyr-Tyr-Arg triad for BpfA´s functionality and also indicates that Asp152 plays a
379 more crucial role than His393 in forming a covalent bond with FAD. This also explains
380 why FBO require the addition of FAD to exhibit stronger catalytic activity. The results
381 confirm that BpfA belongs to the 4PO subfamily, featuring the Tyr-Tyr-Arg triad and a
382 conserved FAD-binding domain.

383 **Global survey on the environmental distributions of *bpfA* gene.**

384 Considering that BpfA homologs are predominantly derived from soil microbes
385 (Fig. 3), we conducted a mapping of BpfA reference sequences onto the species-level
386 microbial genomes present in GTDB and SGBs, aiming to investigate the diversity of
387 BpfA throughout the microbial tree of life. Among 153,143 microbial species across 12
388 phyla, BpfA homologs were identified in 1.08% (1652 genomes) of the species. The
389 study revealed that 67.37% of the microbial species potentially harboring the *bpfA* gene
390 remain uncultured (Fig. S9). BpfA was frequently found among Pseudomonadota
391 (70.04%) and Actinomycetota (20.46%) in the bacterial phyla. However, BpfA was not

392 observed in the archaea phyla (Fig. 4A). Notably, the genera *Paraburkholderia*,
393 *Novosphingobium*, and *Sphingobium* emerged as major bacterial taxa containing BpfA,
394 whereas only a few strains within the genus *Microbacterium* harbor this enzyme (Fig.
395 4B). Combining previously reported BPF-degrading strains, we can infer that bacteria
396 carrying the BpfA and involved in BPF degradation are widely distributed across
397 Pseudomonadota and Actinomycetota. These results expand our knowledge of the
398 variety of bacteria carrying BpfA that participate in BPF biodegradation. Grasping the
399 diversity and distribution of these bacteria is essential for elucidating their ecological
400 importance and potential applications.

401 The functional spectrum of BpfA was delineated by mapping its reference
402 sequences with 3304 metagenomic samples from a wide range of global environments.
403 The study found that BpfA exhibits distinct regional distribution patterns (Fig. 4C).
404 Geographically, BpfA homologs is primarily distributed across Asia, North America,
405 and Europe. These homologs are particularly abundant in environments such as
406 cultivated land and forests, which produce large amounts of lignocellulosic waste (such
407 as wheat straw, corn stover, and trees) annually. These wastes are degraded by soil
408 microbes to produce 4-alkylphenols. The biodegradation of 4-alkylphenols in cultivated
409 land and forests may be significantly influenced by bacteria carrying BpfA. In contrast,
410 in environments with less vegetation and tree cover, such as bare land, shrubland, and
411 tundra, the abundance of BpfA homologs is much lower.

412 Theoretically, the gene encoding BpfA-an enzyme capable of efficiently degrading
413 BPF-may have existed in pre-industrial gene pools. In other words, the ancestral gene

414 of *bpfA* could have been present in nature before humans synthesized BPF. This broad
415 substrate specificity indicates that BpfA has evolved the capability to degrade a range
416 of structurally similar compounds, likely stemming from its ancestral enzyme's role in
417 degrading naturally occurring 4-alkylphenols compounds. BpfA's subsequent evolution
418 to degrade the synthetic compound BPF supports the hypothesis that its progenitor
419 existed pre-industrially to metabolize phenolic intermediates. However, it is also
420 possible that there exists a relatively short evolutionary path from an unknown extant
421 gene to the *bpfA* gene identified in current biodegradation pathways. It has been
422 proposed that a novel sequence for an enzyme targeting a synthetic compound (e.g.,
423 BPF) could evolve via the activation of an unused alternative open reading frame within
424 a pre-existing repetitive coding sequence [43]. However, it is important to note that the
425 similarity between BpfA and members of enzyme superfamilies that catalyze other
426 reactions typically does not provide specific insights into the adaptation process to
427 xenobiotic compounds. The sequence similarity between BpfA and other proteins in
428 phylogenetic families is generally less than 55% (Fig. 3), suggesting that the divergence
429 of BpfA from these enzymes likely occurred much earlier than a century ago. Thus, its
430 evolutionary process cannot be simply attributed to the introduction of industrial
431 chemicals such as BPF into the environment. If BpfA and other key enzymes in
432 metabolic pathways had undergone recent mutations, closely related sequences with
433 only a few mutations differing from the current BpfA enzyme should be present in
434 nature. However, to date, no such primitive BpfA enzyme has been found in the NCBI
435 database. This suggests that BpfA may not have evolved through recent mutation events

436 but rather through more complex evolutionary processes, such as gene mutation or
437 recombination, to acquire its ability to degrade BPF.

438 Nevertheless, BpfA not only exhibits high degradative activity against BPF but
439 also shows some activity towards 4-alkylphenols, which are products of lignocellulosic
440 biomass reductive catalytic fractionation (RCF) [44], such as vanillyl alcohol (VA), 4-
441 n-propylguaiacol (4PG), and 4-(methoxymethyl)phenol (4MOP). This broad substrate
442 specificity of BpfA indicates that it has retained the metabolic function for natural
443 phenolic compounds while evolving the capability to degrade BPF. It is precisely this
444 enzymatic promiscuity of BpfA that makes it a potential biocatalyst for converting 4-
445 alkylphenol compounds into valuable phenolic monomers.

446 **Conclusions**

447 Given the widespread use of BPF, the residues of BPF in the environment cannot
448 be overlooked. However, the metabolic degradation process of BPF by microorganisms
449 is currently poorly understood. In this study, we cloned and identified a novel oxidase
450 gene, *bpfA*, from *Microbacterium* sp. F2, which is responsible for catalyzing BPF into
451 DHBP in a series of reactions. BpfA not only exhibits high degradation activity against
452 BPF but also shows certain activity against 4-alkylphenol compounds such as VA, 4PG,
453 and 4MOP. According to our survey of BpfA in the Global Soil MAGs Project
454 metagenome database, BpfA homologs are widely distributed in the environment,
455 especially in the metagenomes of cultivated land and forests, mainly belonging to
456 Pseudomonadota and Actinomycetota. This study deepens our understanding of the
457 microbial degradation mechanism of BPF, revealing the catalytic function of the novel

458 oxidase gene *bpfA* and its distribution pattern in the environment.

Author contributions

C.W., M.Z. and Q.H. conceived and developed the study. C.W., M.Z., Y.H. and Q.H. gathered the data and conducted the analyses. C.W., M.Z. and Q.H. led the writing of the manuscript. Q.L., J.H., K.P., Q.Z. and W.J. contributed critically to the analyses and writing. J.Q., X.Y. and Q.H. directed the study and critically revised the manuscript for important intellectual content. All authors edited the manuscript and approved the final version.

Conflict of Interest

No conflict of interest exits in the submission of this manuscript, and manuscript is approved by all authors for publication.

Acknowledgements

This work was supported by the National Key R&D Program of China (2022YFA0912500), the National Natural Science Foundation of China (32170125 and 32400085), and the Postdoctoral Fellowship Program of CPSF (GZC20231127).

References

1. Lin J, Deng L, Sun M, et al. An *in vitro* investigation of endocrine disrupting potentials of ten bisphenol analogues. Steroids. 2021; 169: 108826.
2. Jiang X, Yin L, Zhang N, et al. Bisphenol A induced male germ cell apoptosis via IFN*β*-XAF1-XIAP pathway in adult mice. Toxicol Appl Pharmacol. 2018; 355: 247-256.
3. Pellerin E, Caneparo C, Chabaud S, Bolduc S, Pelletier M. Endocrine-disrupting effects of bisphenols on urological cancers. Environ Res. 2021; 195: 110485.
4. Kawa IA, Akbar Masood, Fatima Q, et al. Endocrine disrupting chemical Bisphenol A and its potential effects on female health. Diabetes Metab Syndr. 2021; 15(3) :803-811.
5. Rahman MS, Pang WK, Ryu DY, Park YJ, Ryu BY, Pang MG. Multigenerational impacts of gestational bisphenol A exposure on the sperm function and fertility of male mice. J Hazard Mater. 2021; 416: 125791.
6. Chen D, Kannan K, Tan H, et al. Bisphenol analogues other than BPA: environmental occurrence, human exposure, and toxicity-A Review. Environ Sci Technol. 2016;50(11):5438-5453.
7. Yang Y, Lu L, Zhang J, Yang Y, Wu Y, Shao B. Simultaneous determination of seven bisphenols in environmental water and solid samples by liquid chromatography-electrospray tandem mass spectrometry. J Chromatogr A. 2014; 1328: 26-34.
8. Fromme H, Küchler T, Otto T, Pilz K, Müller J, Wenzel A. Occurrence of phthalates and bisphenol A and F in the environment. Water Res. 2002; 36(6): 1429-1438.
9. Yamazaki E, Yamashita N, Taniyasu S, et al. Bisphenol A and other bisphenol analogues including BPS and BPF in surface water samples from Japan, China, Korea and India. Ecotoxicol Environ Saf. 2015; 122: 565-572.
10. Yan Z, Liu Y, Yan K, et al. Bisphenol analogues in surface water and sediment from the shallow Chinese freshwater lakes: Occurrence, distribution, source apportionment, and ecological and human health risk. Chemosphere. 2017; 184: 318-328.
11. Zhao B, Tan X, Xue M, et al. Pollution status and distribution characteristics of bisphenols in rivers of Guangyuan city. Environmental Monitoring and Forewarning. 2023; 15(6): 17-23.
12. Niu Y, Wang B, Yang R, et al. Bisphenol Analogues and Their Chlorinated Derivatives in

Breast Milk in China: Occurrence and Exposure Assessment. J Agric Food Chem. 2021; 69(4): 1391-1397.

13. Wang B, Yang Z, Zhang K, et al. Embryonic BPF exposure induces neurodevelopmental and neurobehavioral toxicity by affecting neural stem cell proliferation in *Drosophila*. Environ Pollut. 2025; 369: 125844.

14. Liu Y, Tang W, Ao J, Zhang J, Feng L. Transcriptomics integrated with metabolomics reveals the effect of Bisphenol F (BPF) exposure on intestinal inflammation. Sci Total Environ. 2022; 816: 151644.

15. Wu W, Su Z, Luo C, et al. Bisphenol F (BPF) exposure impairs sperm quality and offspring development in male zebrafish. Toxicol Appl Pharmacol. 2025; 496: 117245.

16. Wei H, Lu H, Zhou J, Wang J, Zhang Q, Zhou Y. Research on the characteristics of bisphenol F degradation and denitrification by *Pseudomonas* sp. HS-2. Ind Water Treatment. 2018; 38(01): 52-56.

17. Lu H, Li JY, Ma LC, et al. Simultaneous removal of bisphenol F and nitrate by a novel isolated strain *Pseudomonas* sp. ZH-FAD. AIP Conf Proc. 2022; 2474: 020003.

18. Inoue D, Hara S, Kashihara M, et al. Degradation of Bis(4-Hydroxyphenyl)methane (bisphenol F) by *Sphingobium yanoikuyae* strain FM-2 isolated from river water. Appl Environ Microbiol. 2008; 74(2): 352-358.

19. Toyama T, Sato Y, Inoue D, et al. Biodegradation of bisphenol A and bisphenol F in the rhizosphere sediment of *Phragmites australis*. J Biosci Bioeng. 2009; 108(2): 147-150.

20. Ren L, Jia Y, Ruth N, et al. Biotransformations of bisphenols mediated by a novel Arthrobacter sp. strain YC-RL1. Appl Microbiol Biotechnol. 2016; 100(4): 1967-1976.

21. Wang C, Li Q, Pan K, et al. Complete mineralization of bisphenol F by a newly isolated *Microbacterium* sp. F2 eliminates its toxicity to sensitive organisms. Int Biodeter Biodegr. 2025; 203: 106109.

22. Brettin T, Davis JJ, Disz T, et al. RASTtk: a modular and extensible implementation of the RAST algorithm for building custom annotation pipelines and annotating batches of genomes. Sci Rep. 2015; 5: 8365.

23. Oberg N, Zallot R, Gerlt JA. EFI-EST, EFI-GNT, and EFI-CGFP: Enzyme Function Initiative (EFI) Web Resource for Genomic Enzymology Tools. J Mol Biol. 2023; 435(14):

532 168018.
533 24. Doncheva NT, Morris JH, Holze H, et al. Cytoscape stringApp 2.0: Analysis and
534 Visualization of Heterogeneous Biological Networks. J Proteome Res. 2023; 22(2): 637-
535 646.
536 25. Kohli DK, Bachhawat AK. CLOURE: Clustal Output Reformatter, a program for
537 reformatting ClustalX/ClustalW outputs for SNP analysis and molecular systematics.
538 Nucleic Acids Res. 2003; 31(13): 3501-3502.
539 26. Tamura K, Stecher G, Kumar S. MEGA11: Molecular Evolutionary Genetics Analysis
540 Version 11. Mol Biol Evol. 2021; 38(7): 3022-3027.
541 27. Ma B, Lu C, Wang Y, et al. A genomic catalogue of soil microbiomes boosts mining
542 of biodiversity and genetic resources. Nat Commun. 2023; 14(1): 7318.
543 28. Hyatt D, Chen GL, Locascio PF, Land ML, Larimer FW, Hauser LJ. Prodigal:
544 prokaryotic gene recognition and translation initiation site identification. BMC
545 Bioinformatics. 2010; 11: 119.
546 29. Parks DH, Chuvochina M, Rinke C, Mussig AJ, Chaumeil PA, Hugenholtz P. GTDB:
547 an ongoing census of bacterial and archaeal diversity through a phylogenetically
548 consistent, rank normalized and complete genome-based taxonomy. Nucleic Acids
549 Res. 2022; 50(D1): D785-D794.
550 30. Tang ST, Song XW, Chen J, et al. Widespread Distribution of the *arsO* gene confers
551 bacterial resistance to environmental antimony. Environ Sci Technol. 2023; 57(39):
552 14579-14588.
553 31. Dijkman WP, de Gonzalo G, Mattevi A, Fraaije MW. Flavoprotein oxidases: classification
554 and applications. Appl Microbiol Biotechnol. 2013; 97(12): 5177-5188.
555 32. Copp JN, Anderson DW, Akiva E, Babbitt PC, Tokuriki N. Exploring the sequence, function,
556 and evolutionary space of protein superfamilies using sequence similarity networks and
557 phylogenetic reconstructions. Methods Enzymol. 2019; 620: 315-347.
558 33. Guo Y, Alvigini L, Trajkovic M, et al. Structure- and computational-aided engineering of an
559 oxidase to produce isoeugenol from a lignin-derived compound. Nat Commun. 2022; 13(1):
560 7195.
561 34. Ewing TA, Nguyen QT, Allan RC, et al. Two tyrosine residues, Tyr-108 and Tyr-503, are

562 responsible for the deprotonation of phenolic substrates in vanillyl-alcohol oxidase. J Biol
563 Chem. 2017; 292(35): 14668-14679.
564 35. Kim J, Fuller JH, Cecchini G, McIntire WS. Cloning, sequencing, and expression of the
565 structural genes for the cytochrome and flavoprotein subunits of *p*-cresol methylhydroxylase
566 from two strains of *Pseudomonas putida*. J Bacteriol. 1994;176(20):6349-6361.
567 36. Leferink NG, Heuts DP, Fraaije MW, van Berkel WJ. The growing VAO flavoprotein family.
568 Arch Biochem Biophys. 2008; 474(2): 292-301.
569 37. Ewing TA, Fraaije MW, Mattevi A, van Berkel WJH. The VAO/PCMH flavoprotein family.
570 Arch Biochem Biophys. 2017; 632: 104-117.
571 38. Gygli G, de Vries RP, van Berkel WJH. On the origin of vanillyl alcohol oxidases. Fungal
572 Genet Biol. 2018; 116: 24-32.
573 39. Fraaije MW, van den Heuvel RH, van Berkel WJ, Mattevi A. Covalent flavinylation is
574 essential for efficient redox catalysis in vanillyl-alcohol oxidase. J Biol Chem. 1999; 274(50):
575 35514-35520.
576 40. Sambrook, J.; Fritsch, E. F.; Maniatis, T. Molecular cloning: a laboratory manual
577 (No. Ed. 2), Cold spring harbor laboratory press. 1989.
578 41. Fraaije MW, van Berkel WJ. Catalytic mechanism of the oxidative demethylation of 4-
579 (methoxymethyl)phenol by vanillyl-alcohol oxidase. Evidence for formation of a *p*-quinone
580 methide intermediate. J Biol Chem. 1997; 272(29): 18111-18116.
581 42. Nguyen QT, de Gonzalo G, Binda C, Rioz-Martínez A, Mattevi A, Fraaije MW. Biocatalytic
582 Properties and Structural Analysis of Eugenol Oxidase from *Rhodococcus jostii* RHA1: A
583 Versatile Oxidative Biocatalyst. Chembiochem. 2016; 17(14): 1359-1366.
584 43. Ohno S. Birth of a unique enzyme from an alternative reading frame of the preexisted,
585 internally repetitious coding sequence. Proc Natl Acad Sci U S A. 1984; 81(8): 2421-2425.
586 44. Renders T, Van den Bossche G, Vangeel T, Van Aelst K, Sels B. Reductive catalytic
587 fractionation: state of the art of the lignin-first biorefinery. Curr Opin Biotechnol. 2019; 56:
588 193-201.
589 45. Zhang M, Bai X, Li Q, et al. Functional analysis, diversity, and distribution of carbendazim
590 hydrolases MheI and CbmA, responsible for the initial step in carbendazim degradation.
591 Environ Microbiol. 2022; 24(10): 4803-4817.

592 **Figure Legends**

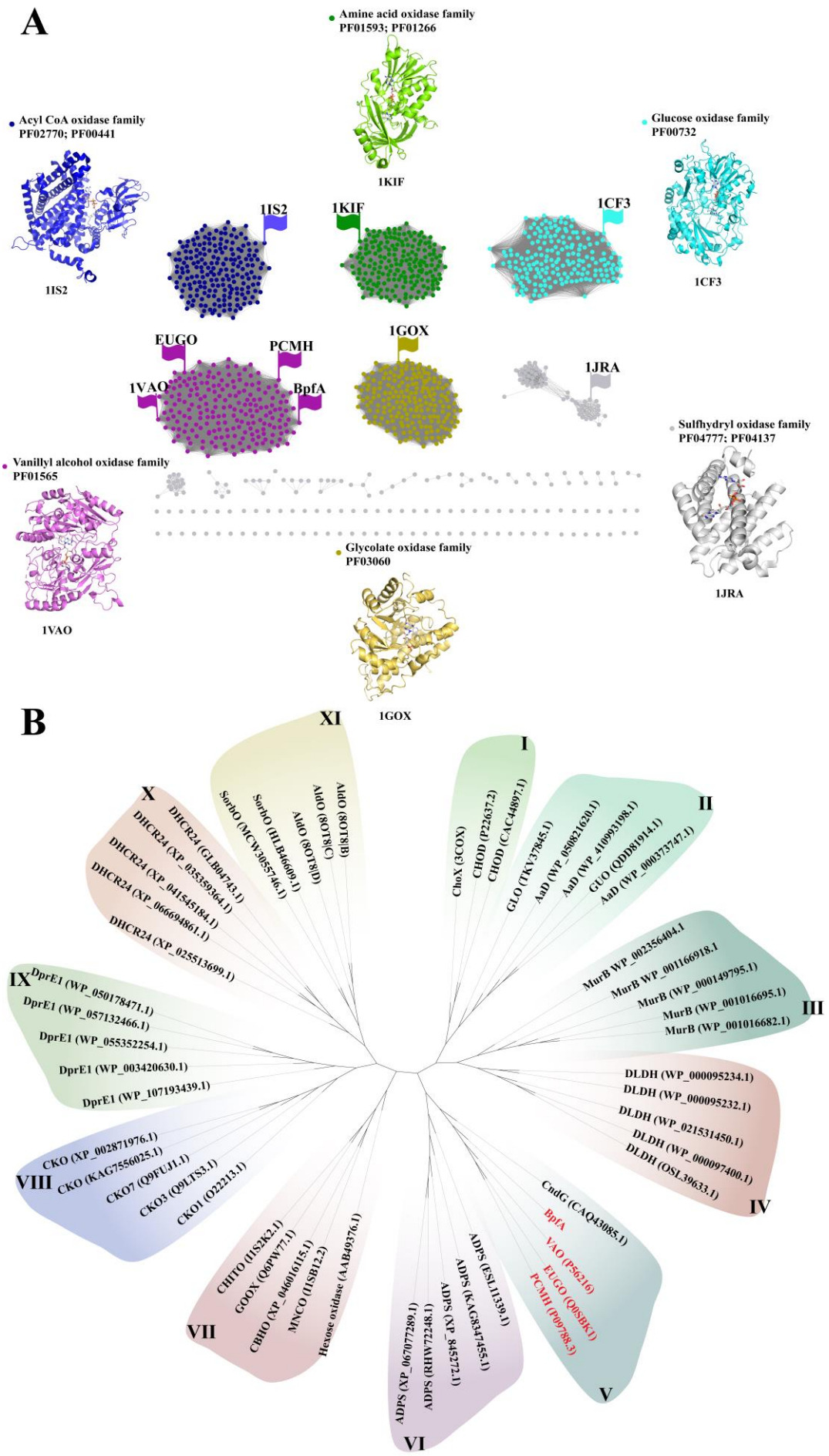
A
Amine acid oxidase family
PF01593; PF01266
1KIF
Acyl CoA oxidase family
PF02770; PF00441
1IS2
Glucose oxidase family
PF00732
1CF3
1IS2
1KIF
1CF3
EUGO
PCMH
1VAO
BpfA
1GOX
1JRA
Sulfhydryl oxidase family
PF04777; PF04137
Vanillyl alcohol oxidase family
PF01565
1VAO
Glycolate oxidase family
PF03060
1GOX
1JRA
B
XI
AldO (8OT8|B)
AldO (8OT8|C)
AldO (8OT8|D)
SorbO (HLB46609.1)
SorbO (MCW3055746.1)
X
DHCR24 (GLB04743.1)
DHCR24 (XP_035359364.1)
DHCR24 (XP_041545184.1)
DHCR24 (XP_066694861.1)
DHCR24 (XP_025513699.1)
I
ChoX (3COX)
CHOD (P22637.2)
CHOD (CAC44897.1)
II
GLO (TKV37845.1)
AaD (WP_050821620.1)
AaD (WP_410993198.1)
GUO (QDD81914.1)
AaD (WP_000373747.1)
III
MurB WP_002356404.1
MurB WP_001166918.1
MurB (WP_000149795.1)
MurB (WP_001016695.1)
MurB (WP_001016682.1)
IX
DprE1 (WP_050178471.1)
DprE1 (WP_057132466.1)
DprE1 (WP_055352254.1)
DprE1 (WP_003420630.1)
DprE1 (WP_107193439.1)
IV
DLDH (WP_000095234.1)
DLDH (WP_000095232.1)
DLDH (WP_021531450.1)
DLDH (WP_000097400.1)
DLDH (OSL39633.1)
VIII
CKO (XP_002871976.1)
CKO (KAG7556025.1)
CKO7 (Q9FUJ1.1)
CKO3 (Q9LTS3.1)
CKO1 (O22213.1)
V
CndG (CAQ43085.1)
BpfA
VAO (P56216)
EUGO (Q0SBK1)
PCMH (P09788.2)
VII
CHITO (I1S2K2.1)
GOOX (Q6PW77.1)
CBHO (XP_046016115.1)
MNCO (I1SB12.2)
Hexose oxidase (AAB49376.1)
VI
ADPS (XP_067077289.1)
ADPS (RHW72248.1)
ADPS (XP_845272.1)
ADPS (KAG8347455.1)
ADPS (ESL11339.1)

Fig. 1. (A) Sequence similarity network (SSN) for representative flavoprotein oxidase superfamily in the NCBI Non-redundant Protein Sequences Database. Each item is arranged in the following order: protein name and accession number. The around are shown the structures of representative members of the different flavin-dependent oxidases with the FAD or FMN cofactor highlighted in gold. (B) Phylogenetic analysis of BpfA with the sequences of other members of the VAO flavoprotein family. I: cholesterol oxidases subfamily; II: aldonolactone oxidoreductases subfamily; III: MurBs subfamily; IV: α-Hydroxy acid dehydrogenases subfamily; V: 4-phenol oxidizing subfamily; VI: alkyl-dihydroxyacetone phosphate synthases subfamily; VII: BBE-like subfamily; VIII: cytokinin dehydrogenases subfamily; IX: DprE1s subfamily; X: sterol reductases subfamily; XI: alditol oxidases subfamily.

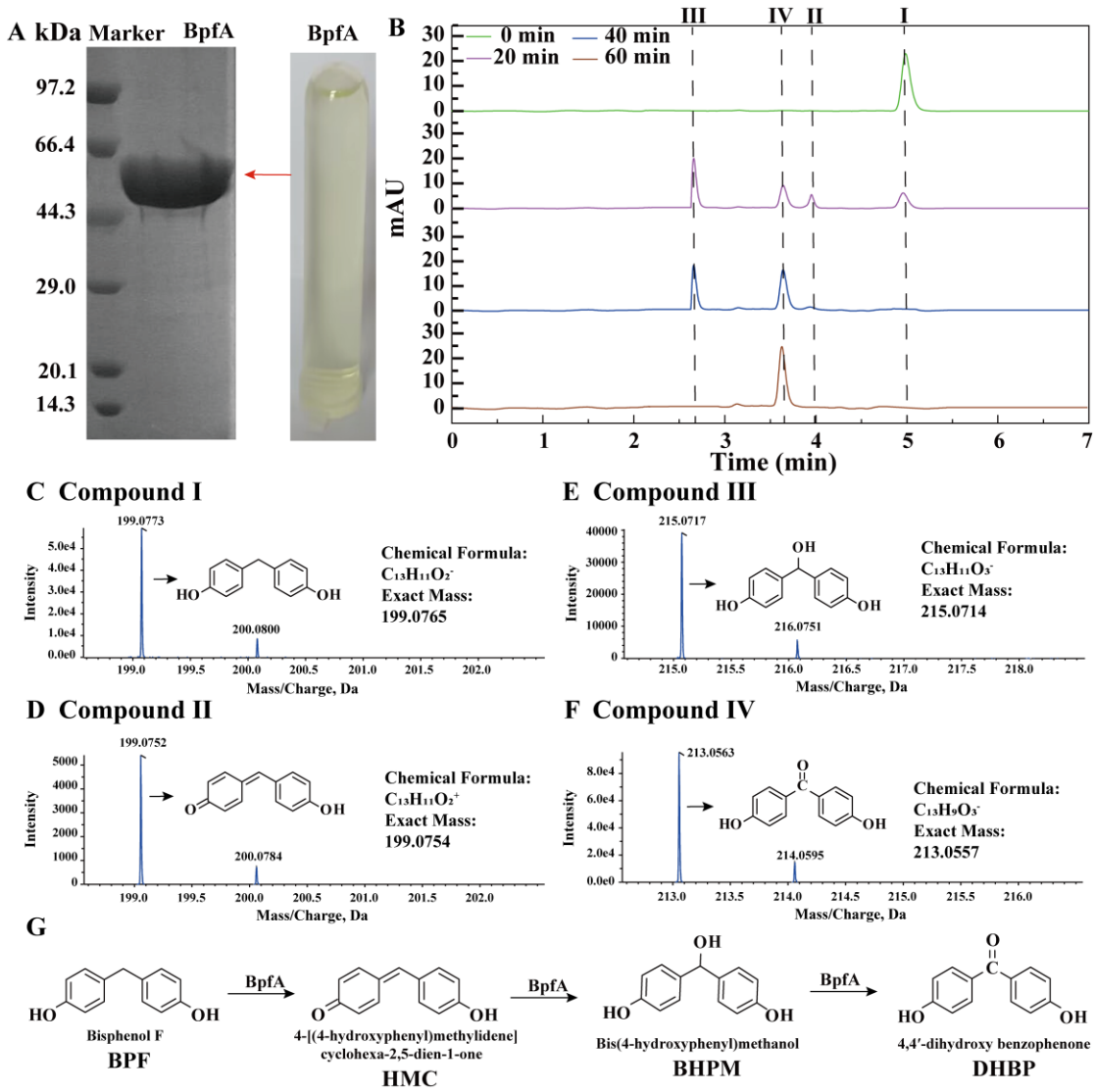

Fig. 2. HPLC-MS analysis of BPF products treated with BpfA. (A) SDS-PAGE analysis of the purified BpfA. (B) HPLC analysis of metabolites that appeared during the conversion of BPF by purified BpfA. (C) HPLC-MS analysis of compound I (*m/z* 199.0773 $[M-H]^-$), which was identified as BPF. (D) HPLC-MS analysis of compound II (*m/z* 199.0752 $[M+H]^+$), which was identified as HMC. (E) HPLC-MS analysis of compound III (*m/z* 215.0717 $[M-H]^-$), which was identified as BHPM. (F) HPLC-MS analysis of compound IV (*m/z* 213.0563 $[M-H]^-$), which was identified as DHBP. (G) The proposed metabolic pathway of BPF degradation by BpfA. BPF: bisphenol F; HMC: 4-[(4-hydroxyphenyl)methylidene]cyclohexa-2,5-dien-1-one; BHPM: bis (4-

617 hydroxyphenyl) methanol; DHBP: 4,4´-dihydroxybenzophenone.

618

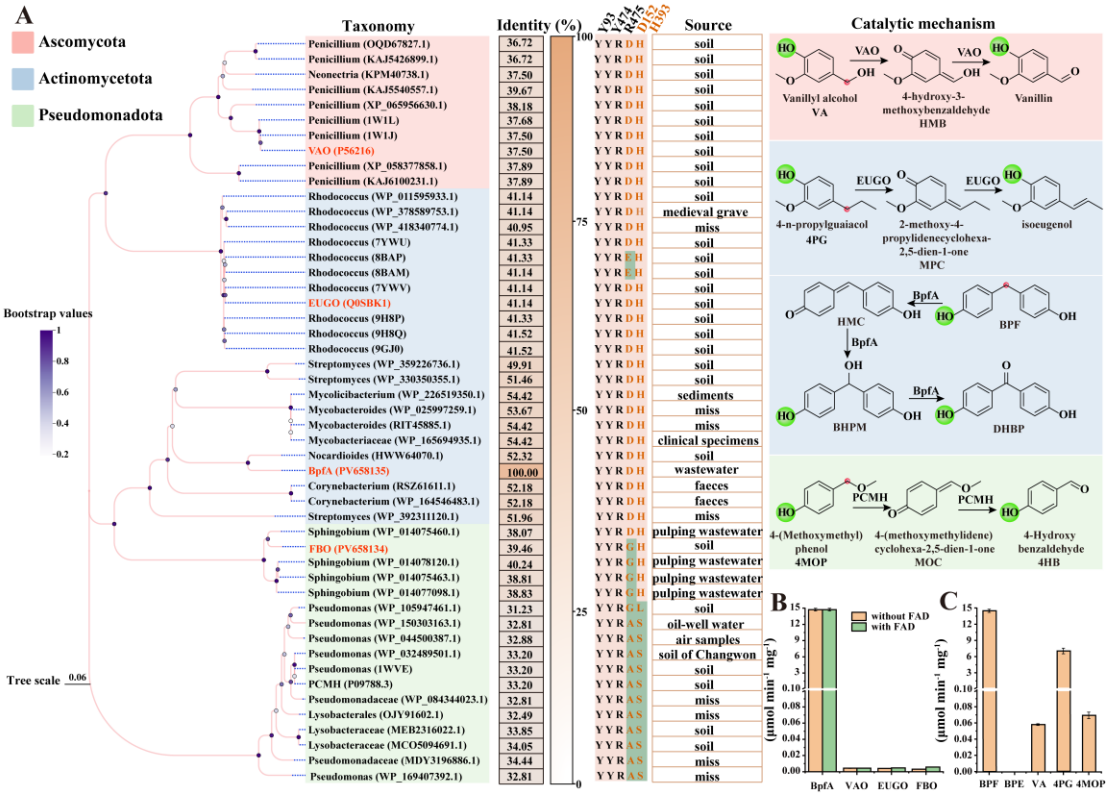

Fig. 3. Bioinformatic and functional analyzes of the 4-phenol oxidizing (4PO) subfamily proteins. (A) Phylogenetic tree of BpfA. The identity of BpfA homologous sequences is indicated on the right side of the phylogenetic tree. The three conserved key amino acid residues (black) and two conserved FAD-binding sites (orange) for each sequence are shown on the right side, and their positions in BpfA are indicated on the top of the columns. The residues with a green background are mutated residues, differing from the conserved residues marked with a pink background. The sources of strains containing BpfA homologous sequences are listed on the right side of the conserved amino acid sequences. On the far right side of the phylogenetic tree detail the catalytic mechanisms of VAO, BpfA, EUGO, and PCMH for their respective substrates. Green spheres represent invariant residues; red spheres indicate the catalytic sites of the reactions. (B) Assessment of the BPF activity of BpfA, VAO, EUGO, and

632 FBO. The data represent the mean values of two replicates using independent enzyme
633 preparation. (C) Assessment of the BPF, BPE, VA, 4PG, and 4MOP enzyme activity of
634 BpfA. The data represent the mean values of two replicates using independent enzyme
635 preparation.
636

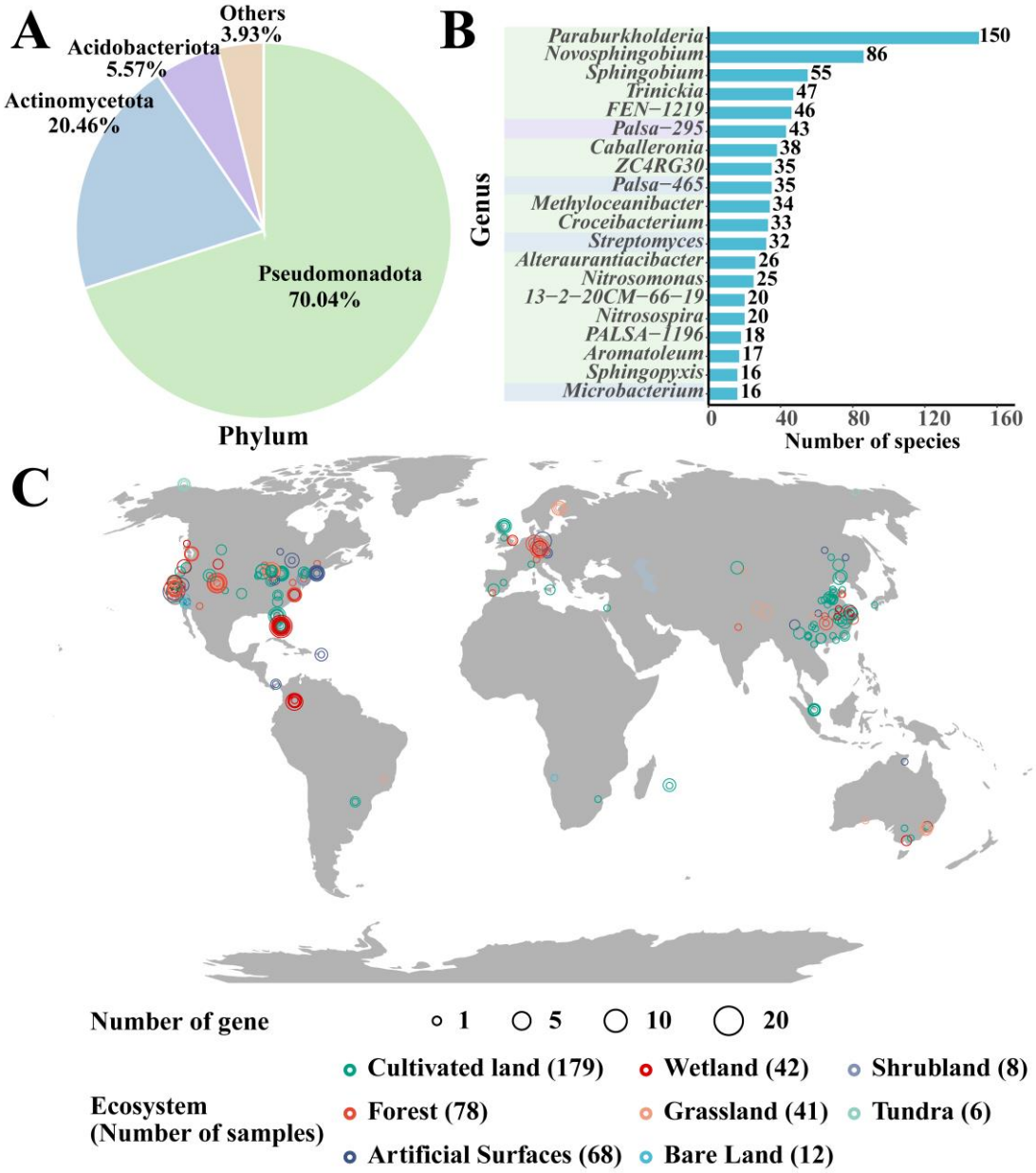

Fig. 4. Microbial classification and distribution pattern of the BpfA in global environments. (A) The number of species that mapped the BpfA across phyla in the domain of bacteria and archaea. (B) The number of species that mapped the BpfA across genera in the domain of bacteria and archaea. (C) Geographic and abundance distribution of the BpfA-harboring bacteria.

Classification

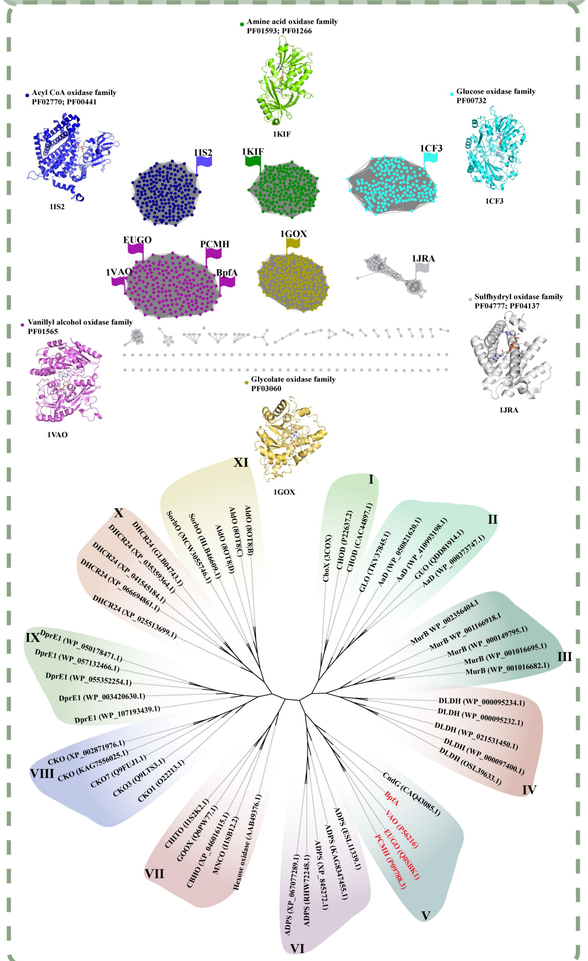

Function

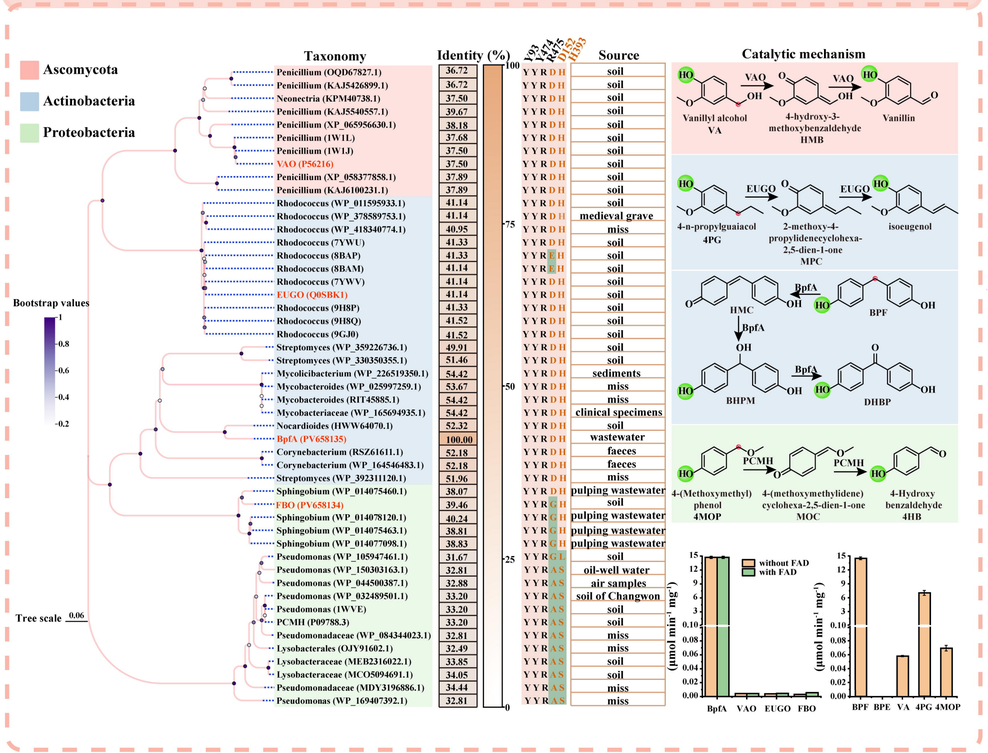

Distribution

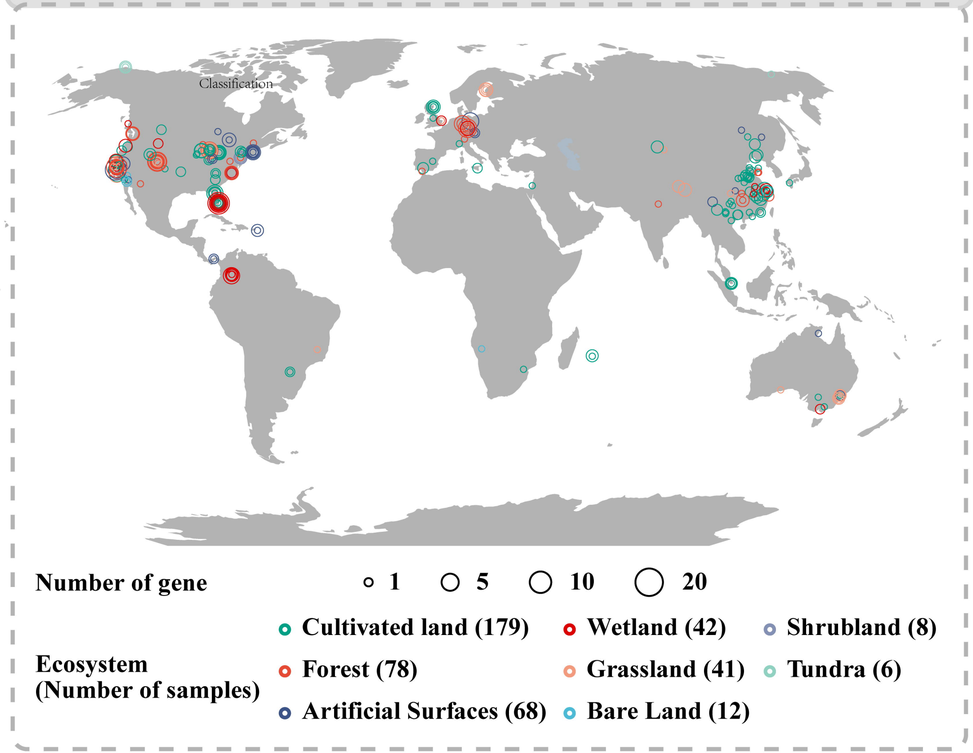

A novel oxidase BpfA